DNA single-strand break repair and spinocerebellar ataxia with axonal neuropathy-1

S F El-Khamisy, Keith Caldecott

Publication date
14-04-2007

Published in
Neuroscience

Link to external publisher version
https://doi.org/10.1016/j.neuroscience.2006.08.048

TDP1 FACILITATES REPAIR OF IONIZING RADIATION-INDUCED DNA SINGLE-STRAND BREAKS

Sherif F. El-Khamisy[1,2], Edgar Hartsuiker[1] and Keith W. Caldecott[1]

[1]Genome Damage and Stability Centre, University of Sussex, Science Park Road, Falmer, Brighton, BN1 9RD, UK

[2]Biochemistry Department, Faculty of Pharmacy, Ain Shams University, P.O.B 11566, Cairo, Egypt

Running title: TDP1 facilitates repair of IR-induced DNA SSBs

Address correspondence to: K.W.C (Tel. +44 1273 877519, Fax. +44 1273 678121, Email: k.w.caldecott@sussex.ac.uk or S.F.E-K (Tel +44 1273 877511, Fax. +44 1273 678121, Email: s.m.f.a.m.el-khamisy@sussex.ac.uk

Abstract

Tyrosyl DNA phosphodiesterase-1 (TDP1) is the gene product mutated in spinocerebellar ataxia with axonal neuropathy1 (SCAN1). SCAN1 is a hereditary ataxia that lacks extra-neurological phenotype, pointing to a critical role for TDP1 in the nervous system. Recently, we showed that TDP1 is associated with the DNA single-strand break (SSBR) repair machinery through an interaction with DNA ligase 3α (Lig3α) and that SCAN1 cells are defective in the repair of chromosomal DNA single-strand breaks (SSBs) arising from abortive Topoisomerase 1 (Top1)-DNA intermediates. Here we demonstrate that TDP1 is also required for the repair of SSBs induced by ionizing radiation (IR), though not measurably for IR-induced DNA double-strand breaks (DSBs). In addition, we provide evidence that abortive Top1 cleavage complexes are processed by the proteasome prior to the action of TDP1 *in vivo*, and we exploit this observation to show that the SSBR defect in SCAN1 following IR reflects, in part at least, the presence of IR-induced protein-DNA cross-links. Finally we show that TDP1 activity at abortive Top1-SSBs is stimulated by XRCC1/Lig3α in vitro. These data expand the type of SSBs processed by TDP1 to include those induced by ionizing radiation, and raise the possibility that TDP1 inhibitors may improve radiotherapy.

1. Introduction

Tens of thousands of DNA single-strand breaks (SSBs) arise in each cell every day [1]. Most if not all the termini at these breaks lack conventional 3'-hydroxyl and 5'-phosphate and their processing is essential for completion of subsequent repair steps. TDP1 is a DNA end processing enzyme, the primary function of which is to hydrolyse the covalent bond between Top1 and the 3'-terminus of DNA in abortive Top1 cleavage complexes [2,3]. During its normal catalytic activity, Top1 generates a "reversible" intermediate known as the cleavage complex, in which Top1 is covalently attached via a tyrosyl residue (human Tyr723) to the 3'-terminus of a single stranded nick [4,5]. These reversible complexes can, however, be

converted into "abortive" intermediates comprised of Top1-associated DNA single- or double-strand breaks by collision with the transcription machinery or with DNA replication forks [6-14]. Steady-state levels of cleavage complexes are increased by the Top1 inhibitor camptothecin (CPT), or by the close proximity of these intermediates to other types of DNA lesions or unusual DNA secondary structures [15-21]. Biochemical and structural data suggest that intact stalled Top1 may not be good substrate for TDP1, implying that a conformational change or partial degradation is needed prior to TDP1 activity [22-24]. TDP1 may also process other types of termini, including 3'-damaged sugar moieties, though these activities have so far only been demonstrated *in-vitro* [25,26]. Mutation in the active site of TDP1 is associated with the human neurodegerative disease Spinocerebellar Ataxia with Axonal Neuropathy-1 (SCAN1) [27]. SCAN1 is typified by cerebellar ataxia and progressive degeneration of the cerebellum, with symptoms restricted to non-dividing neuronal cells. Lymphoblastoid cells (LCLs) from SCAN1 individuals exhibit a defect in the repair of oxidative and CPT-induced SSBs, and TDP1 is intimately associated with the SSBR machinery via direct interaction with DNA Lig3α [28-31].

Ionizing radiation (IR) is widely exploited as a modality for cancer treatment, with cellular radio-resistance being a major unresolved problem. In order to improve radiotherapy, a better understanding of how cells respond to radiation damage is needed. IR induces DNA base damage, SSBs, and DSBs, with the latter being the primary cytotoxic lesion [32-35]. Unrepaired SSBs can be converted into DSBs during DNA replication, raising the possibility that SSBR inhibitors can sensitize certain types of tumors to radiotherapy [36,37]. Whereas the mechanisms by which IR-induced DSBs have been extensively studied *in vivo*, less is known about the repair of IR-induced SSBs. Here, we have assessed the requirement for TDP1 at sites of IR-induced DNA strand breaks using alkaline and neutral comet assays. We report that SCAN1 LCLs, harbouring mutated TDP1, exhibit a measurable delay in the rate of removal of SSBs induced by IR. In contrast, we did not detect a measurable delay in the repair of IR-induced DSBs, using the neutral comet assay. The SSBR defect in SCAN1 cells was attributed, at least in part, to the presence of IR-induced abortive Top1-DNA intermediates. Finally, we report that XRCC1 and DNA Lig3α weakly stimulate TDP1 activity at 3'-phosphotyrosine SSBs, *in vitro*.

2. Materials and Methods

2.1 Cell Lines

Lymphoblastoid cell lines (LCLs) derived from SCAN1 patients and normal individuals have been described previously [27] and were maintained in suspension culture at a density of 2-5X10^5 viable cells/ml in RPMI 1640 supplemented with 15% foetal calf serum (FCS), 2mM L-glutamine, 100U/ml penicillin, and 100μg/ml streptomycin.

2.2 Alkaline comet assays

Cells (~3X10^5 cells/sample) were exposed to γ-irradiation (caesium 137, CammaeII 1000) or treated with CPT as indicated in the appropriate figure legend. Cells were then suspended in pre-chilled PBS and mixed with equal volume of 1.2% low-gelling-temperature agarose (Sigma, type VII) maintained at 42°C. The cell suspension was immediately layered onto pre-chilled frosted glass slides (Chance Propper) pre-coated with 0.6% agarose and maintained in the dark at 4°C until set, and for all further steps. Slides were immersed in pre-chilled lysis buffer (2.5M NaCl, 10mM Tris-HCl, 100mM EDTA pH8.0, 1% Triton X-100, 1% DMSO, pH10) for 1 hr, washed with pre-chilled distilled water (2x10min), and placed for 45 min in pre-chilled alkaline electrophoresis buffer (50mM NaOH, 1mM EDTA, 1% DMSO). Electrophoresis was then conducted at 25V (0.6V/cm) for 25 min, followed by neutralisation in 400 mM Tris-HCl pH7.0 for 1 hr. Finally, DNA was stained with Sybr Green I (1:10,000 dilution in PBS) for 30 min. DNA strand breakage was expressed as "comet tail moment", which is the product of the tail length and the fraction of DNA that has exited the nucleus during electrophoresis [38]. The comet tail moment was measured for at least 100 cells per sample using Comet Assay III software (Perceptive Instruments, UK). Where indicated, cells were either mock-incubated or incubated with 50 μM of the proteosome inhibitor Z-Leu-Leu-Leu-

al (MG132; Sigma) for 2 hr prior to exposure to γ-irradiation or CPT, and during subsequent repair incubations.

2.3 Neutral comet assays

Neutral comet assays were conducted as described [39,40], with some modification. Briefly, following exposure to γ-irradiation, cells were embedded in agarose and layered onto frosted slides as described for the alkaline comet assay. Slides were then immersed in pre-chilled lysis buffer (2.5M NaCl, 10mM Tris-HCl, 100mM EDTA pH8.0, 0.5% Triton X-100, 1% N-lauroylsarcosine, 3% DMSO, pH9.5) for 1.5 hr and then washed with pre-chilled distilled water (2x10min), followed by pre-chilled electrophoresis buffer (300mM sodium acetate, 100mM Tris-HCl, 1% DMSO, pH8.3) (2x10min). Slides were equilibrated in fresh electrophoresis buffer for a further 1 hr and electrophoresis was then conducted in fresh electrophoresis buffer at 25V (0.6V/cm) for 60 min. DNA was stained, visualised, and strand breakage quantified as described for the alkaline comet assay.

2.4 Recombinant proteins

The human ORF encoding TDP1 (Image Clone 3900062, accession no. NM 018319) was obtained from MRC GeneService, UK and amplified using the primers 5'-AGGAATTCAGGAGTATAATGCATCACCATCATCACCATCCGGATCCGATGTCTCAGGAAGGC GATTATGGG-3' (forward) and 5'-ACGAATTCGCTCAGCGTCGACTCAGGAGGGCACCCACATGTTCCC (reverse). Following confirmation by sequencing, the *TDP1* ORF was sub-cloned into the BamH1/EcoR1 sites of pET16B [28] and expression of recombinant histidine-tagged TDP1 (His-TDP) induced in BL21 (DE3) *E. coli* with 1mM IPTG at 30°C for 90 min. Cell pellets (from a 0.5 litre culture) were frozen until required and then re-suspended in 20ml sonication buffer [50mM Hepes pH8, 500mM NaCl, 10% v/v glycerol, 1mM 1,4 dithiothreitol (DTT), 1mM phenylmethylsulphonyl fluoride (PMSF), and 1mM imidazole] and sonicated

for 4x30 sec on ice at 16% power (Soniprep 150, Sanyo). Soluble cell proteins (~100mg total protein) were mixed with 1ml bed volume of NTA-Agarose beads (Qiagen) pre-washed in Wash Buffer (25mM Hepes pH8, 0.1M NaCl, 10% glycerol, 1mM DTT, 1mM imidazole) on ice with gentle stirring for 20 min. The suspension was then added to a Polyprep disposable chromatography column (BioRad) at 4°C and washed with Wash Buffer (1x5 ml) followed by Wash Buffer containing 50mM imidazole (2x5ml). Bound proteins were then eluted with 5ml Elution Buffer (25mM Hepes pH8, 0.1M NaCl, 10% glycerol, 1mM DTT, and 250mM imidazole) and collected in 0.5ml aliquots. Peak fractions were pooled, dialyzed (20mM Hepes pH8, 0.1M NaCl, 1mM DTT, 10% glycerol), and TDP1 further purified by anion exchange chromatochraphy (1.6ml Poros 20 HS column) using a BioCad Chromatography System. Recombinant human histidine-tagged DNA ligase IIIα (Lig3α) and XRCC1 proteins were expressed and purified from pET16BHL3α [41] and pET16BXH [42] respectively essentially as above. Note that in case of Lig3α, lysis and elution were conducted at the same salt concentration (500mM NaCl) throughout to retain solubility. XRCC1 and Lig3α were further purified by gel filteration using a Superdex 200 HR 10/30 column (Pharmacia) at a flow-rate of 0.5ml/min. Aliquots of the purified proteins were snap frozen in liquid nitrogen and stored at -80°C until needed.

2.5 Cell-free SSBR assays.

An 18-mer oligonucleotide (18-Y; 5'-TCCGTTGAAGCCTGCTTT-P-Tyr-3') containing a 3' phosphotyrosyl terminus [2] was a generous gift from H. Nash (National Institute of Mental Health, Bethesda, USA). The 25-mer (5'-GACATACTAACTTGAGCGAAACGGT-3') and 43-mer (3'-TAGGCAACTTCGGACGAAACTGTATGATTGAACTCGCTTTGCC-5') employed to generate a duplex substrate containing a nick with a 3'-phosphotyrosine terminus (see Figure 5A) were synthesized by MWG. The 18Y-mer was phosphorylated by T4 PNK in 25μl reactions containing 5μCi [γ-^{32}P] ATP at 7000Ci/mmol (ICN), and after the removal of unincorporated nucleotides annealed with equimolar amounts of the 25-mer and 43-mer. For repair assays, recombinant proteins were dialyzed in 25mM Hepes

pH8, 130mM KCl, 1 mM DTT and where indicated pre-incubated for 20 min on ice to allow formation of protein complexes. Recombinant proteins were mixed with 25nM duplex substrate (10μl reaction volume) and incubated at 37°C for 1 hr in 25mM Hepes pH8, 130mM KCl, 1mM DTT, 10mM $MgCl_2$, and 1mM ATP. Reactions were stopped by addition of 1X loading buffer (44% deionized formamide, 2.25mM Tris-borate, 0.05mM EDTA, 0.01% xylene cyanol, 1% bromophenol blue), heated at 90°C for 10 min, and repair products fractionated by denaturing electrophoresis at 250V. Repair products were quantified using Molecular Dynamics ImageQuant software (Version 4.2a).

2.6 Detection of Top1-DNA complexes by immunoblotting

Top1 protein-DNA complexes were detected as previously described [43,44]. Briefly, cells ($2X10^6$) were mock treated or incubated in 14 μM camptothecin for 1 hr at 37°C followed by lysis in 1% Sarcosyl, 8 M Guanidine HCl, 30 mM Tris pH 7.5 and 10 mM EDTA. Cell lysates were then incubated at 70°C for 15 minutes to remove all non-covalently bound proteins from DNA. Cell lysates were then loaded on a cesium chloride (CsCl) step gradient (5 ml total volume) and centrifuged at 75,600 g at 25°C for 24 hrs to separate free proteins from DNA. Ten consecutive 0.5 ml fractions were collected and slot blotted onto Hybond-C membrane (Amersham). To ensure equal DNA loading, the DNA concentration in each extract was determined fluorimetrically using PicoGreen (Molecular Probes/Invitrogen). Covalent Top1-DNA complexes were then detected by immunoblotting with anti-Top1 polyclonal antibodies (Abcam, ab3825) and visualised by chemiluminescence. For quantitation, fractions containing Top1-DNA complexes (4-7) were pooled and serial dilutions analysed as described above. Band intensities were quantified using ImageQuant software (GE Healthcare).

3. Results

To examine whether TDP1 is required for the rapid repair of IR-induced SSBs SCAN1 lymphoblastoid cells (LCLs) were exposed to γ-rays (20Gy) and levels of alkali labile sites and DNA strand breaks

quantified using the alkaline comet assay. Although the alkaline comet assay measures both SSBs and DSBs, >95% of breaks induced by IR are SSBs [35]. Consequently, following IR, this assay primarily measures rates of SSBR. Whilst IR induced similar initial levels of DNA strand breakage in normal and SCAN1 cells, the kinetics of removal of these breaks was delayed in the latter (Fig 1A &1B). During a 30 min repair period the level of IR-induced DNA strand breaks in Tdp1+/+ and Tdp1+/- LCLs declined by ~70%, whereas in SCAN1 cells this level declined by only ~40%. After a 60 min repair period SCAN1 cells retained ~40% of their breaks, whereas only 15% remained in normal cells (Fig 1B). These results were consistently observed in three independent SCAN1 cell lines. The SSBR defect in SCAN1 cells was evident not only from the mean tail moments from multiple, averaged, experiments, but also from scatter plots of the raw data from individual experiments (Fig 1C). We conclude from these experiments that the global rate of repair of IR-induced SSBs is decreased in SCAN1 cells.

We next examined whether there is a defect in the repair of IR-induced DSBs in SCAN1 cells, as measured by neutral comet assays. Normal and SCAN1 cells exhibited similar levels of DSBs immediately after irradiation and similar rates of their removal during subsequent repair-incubations (Fig 2A & 2B). In contrast, LCLs obtained from individuals with Lig4 syndrome exhibited delayed kinetics of DSB removal, consistent with their established defect in DNA double-strand break repair [45,46]. It is worth noting that we observed similar results in primary Tdp1-/- mouse neural cells, in which we employed γH2AX immunostaining to quantify rates of DSBR (unpublished observations).

The defect in SSBR observed in SCAN1 cells following IR is much less than that observed following CPT [28]. This most likely reflects that all of the SSBs induced by CPT are substrates for TDP1 whereas only a subset of IR induced lesions may be so. What might be the nature of the IR-induced SSBs that are substrates for TDP1? One possibility is that these are SSBs with 3'-phosphoglycolate (3'-PG) termini, since TDP1 is required to process this type of terminus at single-stranded DNA or at DSBs with 3'-overhangs [25,47]. However, at SSBs, APE1 appears to be the major activity responsible for removing 3'-PG, in vitro at least [48,49]. Alternatively, it is possible that the IR-induced SSBs that are processed by TDP1 are abortive Top1-cleavage complexes, analogous to those induced by CPT. This would be consistent with the observation that the types of sugar damage and base damage that are induced by IR can

stabilise and/or induce Top1 cleavage complexes in a manner similar to CPT [18-21]. To address these possibilities we took advantage of the striking observation that pre-incubation with the proteasome inhibitor MG-132 greatly reduces or ablates the accumulation of SSBs in SCAN1 cells, as measured by the alkaline comet assay, following CPT (Fig 3A). Whereas SCAN1 cells accumulated ~7-fold more SSBs than did normal cells during incubations with CPT in the absence of proteasome inhibitor, pre-incubation with MG-132 reduced the accumulation of CPT-induced SSBs in SCAN1 cells almost to the level observed in normal LCLs (Fig 3A & 3B). This did not reflect an impact of MG-132 on cleavage complex formation because the level of Top1-DNA complexes induced by CPT was largely unaffected (Fig. 3C). Consequently, we conclude that the proteasome is required to convert CPT-induced abortive top1 cleavage complexes into SSBs that can be detected by the alkaline comet assay. These data are entirely consistent with previous observations that the proteasome may be required to process the 'intact' Top1 polypeptide present in abortive cleavage complexes into a truncated-from that can be processed by TDP1 [50-54][22-24].

In light of the above observations, we reasoned that if some or all of the γ ray-induced SSBs that were substrates for TDP1 arose from abortive Top1 cleavage complexes then their persistence in SCAN1 cells would be reduced or ablated by pre-incubation with the MG-132. Alternatively, if the γ ray-induced SSBs reflected breaks induced directly by IR, then MG-132 should not impact on their persistence. We thus exposed normal and SCAN1 cells to γ rays (20 Gy) with or without prior incubation with MG-132 and quantified the level of DNA strand breaks following 30 min and 60 min repair periods, in the presence or absence of MG-132 (Fig 4A). Whereas pre-incubation with MG-132 did not impact on the level of IR-induced strand breaks in normal cells, it decreased the level of breaks present after a 30-60 min repair period in SCAN1 cells by approximately half (Fig 4A & 4B). These data provide compelling evidence that the SSBR defect observed in SCAN1 LCLs following IR reflects, in part at least, SSBs arising indirectly through formation of abortive Top1 cleavage complexes.

The observations reported here and previously [28,30,31] demonstrate that Top1-associated SSBs are TDP1 substrates in cells. However, *in vitro* studies suggest that SSBs are poor substrates for TDP1

compared to single-stranded oligomers or DSBs. We thus examined whether the established association of TDP1 with the XRCC1/DNA Lig3α complex [28,30] might affect its activity at Top1-associated SSBs. The activity of TDP1 was therefore compared in the presence and absence of recombinant human DNA XRCC1/Lig3α using a synthetic 18-mer oligonucleotide containing a SSB with a 3'-phosphotyrosine-linked terminus ("18-Y") to mimic the type of terminus processed by TDP1 within a Top1-associated SSB [2] (Fig 5A, top). TDP1 activity was indicated in these experiments by conversion of the 18-Y substrate to a product that contains a 3'-phosphate (18-P), which consequently has increased electrophoretic mobility (Fig 5A, bottom). Based on this titration experiment, a limiting concentration of TDP1 (1nM) was chosen for further analysis, and was incubated with serial dilutions (0.5, 1, or 2nM) of the indicated recombinant proteins or BSA, and with 18-Y substrate for 60 min at 37°C (Fig 5B). Incubation with TDP1 and BSA resulted in formation of significant amounts 18-mer product (Fig 5B, lanes 1-4). However, the additional presence of DNA Lig3α weakly stimulated the reaction (Fig 5B; lanes 5-7) and the additional presence of XRCC1 stimulated the reaction further (Fig 5B; compare lanes 2-4 with lanes 11-13). We did not observe stimulation when XRCC1 was added alone (Fig 5B; lanes 8-10), nor did we detect repair if TDP1 was omitted from the reaction (data not shown). Similar results were observed if TDP1, BSA, Lig3α, and/or XRCC1 were mixed in equimolar ratios and then titrated into reactions containing the 18-Y substrate (Fig.5C&D). We conclude from these experiments that XRCC1/DNA Lig3α complex stimulates TDP activity on tyrosine-associated SSBs.

4. Discussion

The results presented suggest that TDP1 is required for normal global rates of SSBR following IR. In contrast, we did not detect a defect in the rate of repair of IR-induced DSBs, though we cannot rule out a defect in the repair of a subset of DSBs too small to be detected by the neutral comet assay or by γ-H2AX assays (data presented here and unpublished observations). The favoured substrate for TDP1 is a 3'-terminus covalently linked through a phosphodiester bond to the active site tyrosine of Top1 peptide. To

better understand the nature of the defect in repair of IR-induced SSBs in SCAN1 cells we attempted to distinguish between Top1-associated SSBs and other types of SSBs, *in vivo*. To achieve this we exploited our observation that the proteosome inhibitor MG-132 greatly reduced detection of CPT-induced Top1-associated SSBs by the alkaline comet assay. We interpret this observation to indicate that alkaline comet assays do not detect 'intact' Top1 cleavage complexes, but only those that have been converted into 'true' DNA strand breaks by Top1 degradation or denaturation. This is consistent with the hypothesis that TDP1 activity at SSBs occurs after Top1 in abortive cleavage complexes has been denatured or proteolytically degraded [22,53]. This is most likely necessary during the repair of abortive Top1-cleavage complexes because the DNA-tyrosyl linkage is buried deep within intact Top1 and thus inaccessible to TDP1 [23,24]. Strikingly, we found that MG-132 reduced the level of IR-induced strand breaks remaining in SCAN1 cells after 30 min and 60 min repair periods by approximately half, as measured by alkaline comet assays. This suggests that at least half of the IR-induced breaks that persisted in SCAN1 cells in these experiments were peptide-linked, resulting most likely from Top1-cleavage complexes that were stabilised or trapped by other types of IR-induced lesions [17-21,55,56]. This conclusion is consistent with the observations that Top1-DNA cross-links are induced in HeLa cells by oxidative DNA damage and that Top1-deficient murine leukaemia cells and budding yeast are more resistant to oxidative damage than their wild-type counterparts [57].

The nature of the IR-induced SSBs that persisted in SCAN1 cells in the presence of proteosome inhibitor is unclear. It is possible that these too are Top1-associated breaks, because MG-132 did not completely prevent the accumulation of CPT-induced breaks in SCAN1 cells, despite this Top1 inhibitor inducing DNA breaks exclusively via stabilisation of Top1-cleavage complexes [58-60]. Alternatively, the MG-132 'resistant' breaks that persisted in SCAN1 cells following IR may reflect breaks induced directly by this agent, since TDP1 can process a variety of other types of termini *in vitro*, including 3'-phosphohistidine, 3'-phosphoglycolate, 3'-abasic sites, and 3'-biotin, and even some types of 5'-termini [25,26,47,61]. 3'-phosphoglycolate termini are of particular relevance, since these are present at ~30% of γ-ray induced breaks [62]. Although purified TDP1 is ~100-fold less active on 3'-phosphoglycolate compared to 3'-phosphtyrosyl [25], the repair of protruding 3'-PG at the termini of

DSBs by human cell extracts is entirely dependent on TDP1 [47]. However, whether this is true in vivo is unclear, because SCAN1 LCLs exhibit only very mild radiosensitivity [47], and in the experiments reported here we failed to detect a measurable difference in the rate of DSBR following IR in SCAN1 LCLs, using the neutral comet assay. Moreover, with respect to SSBs, cell-free assays suggest that the processing of 3'-phosphoglycolate is largely attributed to APE1 [48], though whether this is true in vivo is not known.

The observation that TDP1 is required for the rapid removal of SSBs created by IR has important clinical implications. In particular, along with our previous experiments employing H_2O_2 [63], the data presented here provide an attractive explanation for the patho-physiology of SCAN1. Reactive oxygen species are most likely a major source of endogenous SSBs, particularly within the brain which consumes approximately one quarter of inhaled oxygen and possesses relatively low levels of antioxidant enzymes [64]. Consequently, DNA repair mechanisms that remove oxidative DNA damage are likely to be critical for maintaining genetic integrity in the nervous system. It is also tempting to speculate that TDP1-dependent SSBR may impact on normal aging. For example, the levels of 8-oxoguanine, a common product of oxidative stress that can trap Top1 cleavage complexes, are markedly elevated in the promoters of many genes that become down-regulated in an age-dependent manner, suggesting that there is increased oxidative stress and thus increased demand for TDP1-dependent SSBR in aged cells [65]. The results described here also highlight the possible advantage of inhibiting TDP1 during radiotherapy. TDP1 inhibitors may improve cell killing by radiotherapy, particularly in tumors that possess elevated levels of TDP1 activity. Interestingly, increased TDP1 levels and activity have been recently reported in non-small cell lung cancer [66].

TDP1 is highly conserved among species, with an extended amino terminus in human TDP1 that is either absent or poorly conserved in lower eukaryotes [67]. This amino terminus is dispensable for enzymatic activity, and instead appears to serve a regulatory function. For example, this domain is necessary for stimulation of TDP1 by Mn^{2+} [68], and for its association with the SSBR machinery via direct interaction with DNA Lig3α [28]. *In vitro* studies suggest that nicks are poor substrates for TDP1, compared to single-stranded termini or blunt-end substrates [49,69]. However, TDP1 is clearly a

component of the SSBR machinery and is operating at SSBs in cells [28,30,31]. These observations may in part be reconciled by our observation that TDP1 activity was weakly stimulated on Top1 associated SSBs in vitro in the presence of XRCC1/Lig3∝. This stimulation was observed primarily at low enzyme concentration, when levels of TDP1 were limiting. These observations are consistent with the finding that nuclear extracts from rodent cells lacking XRCC1/Lig3∝ show decreased TDP1 activity [30].

In summary, this work provides the first evidence for a requirement for TDP1 for the rapid repair of IR-induced DNA SSBs. Pharmacologic inhibition of TDP1 may therefore be an efficient strategy for sensitizing certain types of tumours to radiotherapy.

Figure Legends

Figure 1 Defective repair of ionizing radiation-induced DNA single-strand breaks in SCAN1 cells. Lymphoblastoid cells derived from SCAN1 patients (1635, 1662, and 1664) homozygous for the TDP1 mutation H493R, or from a heterozygous (1670) or normal individuals (1646, 1688, and 702), were exposed to γ-ray (20Gy) in complete medium on ice (RO), and then incubated at 37°C for 30 min (R30) or 60 min (R60) repair periods. Cells were then washed with pre-chilled PBS and subjected to alkaline comet assays. **(A)** Mean tail moments were quantified for 100 cells/sample/experiment and data are the average of three independent experiments (±SEM). *Top*, representative mock-treated (-IR) or γ-irradiated (+IR; 20Gy) 1688 cells in the alkaline comet assay. **(B)** The mean fraction of DNA strand breaks remaining (±SEM) at the indicated time points. Asterisks denote statistically significant ($P < 0.05$; t-test) differences between SCAN1 and normal histograms at the indicated time points. **(C)** Representative scatter plots from one of the experiments included in Panel A, showing comet tail moments of 100 individual cells per sample (cells numbered from 0-100) at the time points indicated.

Figure 2 Repair of ionizing radiation-induced DNA double-strand breaks in SCAN1 cells. Wild-type (1646), SCAN1 (1635), and Lig4 syndrome (NBS2304) lymphoblastoid cells were exposed to γ-ray (20Gy) in complete medium on ice (RO) and then incubated at 37°C for 60 min (R60), 180 min (R180), or 360 min (R360) repair periods. Cells were then washed with pre-chilled PBS and subjected to neutral comet assays. **(A)** Mean tail moments were quantified for 100 cells/sample/experiment and data are the average of three independent experiments (±SEM). **(B)** The mean fraction (±SEM) of γ-ray induced DSBs remaining at the indicated time points.

Figure 3 Reduced levels of CPT-induced Strand Breaks in SCAN1 cells pre-treated with the proteasome inhibitor MG-132. (A) Wild-type (1646) and SCAN1 (1635) lymphoblastoid cells were

incubated with 14 μM camptothecin for 1 hr at 37°C with (CPT+PI) or without (CPT) prior incubation with 50 μM of the proteosome inhibitor MG132 (PI) for 2 hr at 37°C. Cells were then washed with pre-chilled PBS and subjected to alkaline comet assays to measure DNA strand breaks. Mean tail moments were calculated from 100 cells/sample/experiment and data are the average of three independent experiments (±SEM). **(B)** Representative scatter plots, from one of the experiments presented in panel A, showing 100 individual comet tail moments per sample (cells numbered from 0-100). **(C)** *Left,* The indicated cells were mock-treated ("-") or incubated in 14 μM camptothecin for 1 hr at 37°C ("CPT") in the absence ("-PI") or presence ("+PI") of MG-132 proteasome inhibitor, and then lysed and fractionated on CsCl gradients. Fractions containing Top1-DNA complexes (#7-10) were identified by immunobloting and pooled. 2-fold serial dilutions (three dilutions, shown top to bottom) of these fractions slot blotted onto nitrocellulose and immunoblotted with anti-Top1 polyclonal antibodies (ab-3825). *Right*, Top1 cleavage complexes (fold-increase over background) were quantified for each of the serial dilutions depicted in the left panel, using ImageQuant software, and the mean value plotted (+/- 1S.D). Data are from one representative experiment of three independent experiments conducted.

Figure 4 Reduced levels of IR-induced strand breaks in SCAN1 cells pre-treated with the proteosome inhibitor MG132. Wild-type (1646) or SCAN1 (1635) lymphoblastoid cells were mock incubated (-PI) or incubated with 50 μM of the proteosome inhibitor MG132 (+PI) for 2 hr at 37°C, exposed to γ-rays (20Gy) in complete medium on ice (RO), and then incubated at 37°C for 30 min (R30) or 60 min (R60) repair periods, in the presence or absence of MG132, as indicated. Cells were then washed with pre-chilled PBS and subjected to alkaline comet assays. **(A)** Mean tail moments were quantified for 100 cells/sample/experiment and data are the average of three independent experiments (±SEM). **(B)** The mean fraction of DNA strand breaks remaining (±SEM) at the indicated time points. P values indicate that the difference between mock-treated (-PI) and MG-132-treated (+PI) SCAN1 cells is statistically significant (T-test).

Figure 5 DNA Lig3α/XRCC1 enhances the activity of TDP1 at Top1-associated SSBs, *in-vitro*. (A) *Top*, A single stranded 18-mer oligonucleotide with 3'-phosphotyrosine residue (18Y) was employed to generate a duplex substrate with a nick that contains a 3'-phosphotyrosine terminus, mimicking a Top1-associated SSB (inset). *Bottom*, 25 nM 18-Y substrate was incubated with 1-32 nM recombinant human TDP1 for 1 hr at 37°C. Reaction products were fractionated by denaturing polyacrylamide gel electrophoresis and examined by autoradiography. **(B)** 18-Y substrate was incubated with a limiting concentration of TDP1 (1 nM) in the presence of increasing concentrations (0.5, 1, and 2 nM) of each of the indicated proteins for 1 hr at 37°C. Reaction products were fractionated by denaturing polyacrylamide gel electrophoresis and examined by autoradiography. A representative experiment from three independent experiments is shown. **(C)** *Left*, the 18-Y substrate was incubated in the absence (-) or presence of 1, 2, or 4 nM of each of the indicated recombinant human proteins for 1 hr at 37°C. Note that in lanes 5-7, BSA was present at 2, 4, or 8 nM to substitute for the absence of both XRCC1 and Lig3α. Reaction products were fractionated by denaturing polyacrylamide gel electrophoresis and examined by autoradiography. *Right*, 18-P product was quantified by ImageQuant software and expressed as the fraction (%) of total labelled oligonucleotide duplex. Data are the mean (± SEM) of three independent experiments.

References

[1] **T. Lindahl Instability and decay of the primary structure of DNA, Nature 362 (1993) 709-715.**

[2] **S.W. Yang, A.B. Burgin, Jr., B.N. Huizenga, C.A. Robertson, K.C. Yao and H.A. Nash A eukaryotic enzyme that can disjoin dead-end covalent complexes between DNA and type I topoisomerases, Proc Natl Acad Sci U S A 93 (1996) 11534-11539.**

[3] **J.J. Pouliot, K.C. Yao, C.A. Robertson and H.A. Nash Yeast gene for a Tyr-DNA phosphodiesterase that repairs topoisomerase I complexes, Science 286 (1999) 552-555.**

[4] **J.J. Champoux and R. Dulbecco An activity from mammalian cells that untwists superhelical DNA--a possible swivel for DNA replication (polyoma-ethidium bromide-mouse-embryo cells-dye binding assay), Proc Natl Acad Sci U S A 69 (1972) 143-146.**

[5] **L. Stewart, M.R. Redinbo, X. Qiu, W.G. Hol and J.J. Champoux A model for the mechanism of human topoisomerase I, Science 279 (1998) 1534-1541.**

[6] **K. Avemann, R. Knippers, T. Koller and J.M. Sogo Camptothecin, a specific inhibitor of type I DNA topoisomerase, induces DNA breakage at replication forks, Mol Cell Biol 8 (1988) 3026-3034.**

[7] **C. Holm, J.M. Covey, D. Kerrigan and Y. Pommier Differential requirement of DNA replication for the cytotoxicity of DNA topoisomerase I and II inhibitors in Chinese hamster DC3F cells, Cancer Res 49 (1989) 6365-6368.**

[8] **Y.H. Hsiang, M.G. Lihou and L.F. Liu Arrest of replication forks by drug-stabilized topoisomerase I-DNA cleavable complexes as a mechanism of cell killing by camptothecin, Cancer Res 49 (1989) 5077-5082.**

[9] **A.J. Ryan, S. Squires, H.L. Strutt and R.T. Johnson Camptothecin cytotoxicity in mammalian cells is associated with the induction of persistent double strand breaks in replicating DNA, Nucleic Acids Res 19 (1991) 3295-3300.**

[10] **D. Strumberg, A.A. Pilon, M. Smith, R. Hickey, L. Malkas and Y. Pommier Conversion of topoisomerase I cleavage complexes on the leading strand of ribosomal DNA into 5'-phosphorylated DNA double-strand breaks by replication runoff, Mol Cell Biol 20 (2000) 3977-3987.**

[11] **W. Adam, C.R. Saha-Moller, A. Schonberger, M. Berger and J. Cadet Formation of 7,8-dihydro-8-oxoguanine in the 1,2-dioxetane-induced oxidation of calf thymus DNA: evidence for photosensitized DNA damage by thermally generated triplet ketones in the dark, Photochem Photobiol 62 (1995) 231-238.**

[12] **C. Bendixen, B. Thomsen, J. Alsner and O. Westergaard Camptothecin-stabilized topoisomerase I-DNA adducts cause premature termination of transcription, Biochemistry 29 (1990) 5613-5619.**

[13] **J. Wu and L.F. Liu Processing of topoisomerase I cleavable complexes into DNA damage by transcription, Nucleic Acids Res 25 (1997) 4181-4186.**

[14] **P.E. Kroeger and T.C. Rowe Interaction of topoisomerase 1 with the transcribed region of the Drosophila HSP 70 heat shock gene, Nucleic Acids Res 17 (1989) 8495-8509.**

[15] **E. Kjeldsen, J.Q. Svejstrup, Gromova, II, J. Alsner and O. Westergaard Camptothecin inhibits both the cleavage and religation reactions of eukaryotic DNA topoisomerase I, J Mol Biol 228 (1992) 1025-1030.**

[16] **Y. Pommier, P. Pourquier, Y. Fan and D. Strumberg Mechanism of action of eukaryotic DNA topoisomerase I and drugs targeted to the enzyme, Biochim Biophys Acta 1400 (1998) 83-105.**

[17] **Y. Pommier, G.S. Laco, G. Kohlhagen, J.M. Sayer, H. Kroth and D.M. Jerina Position-specific trapping of topoisomerase I-DNA cleavage complexes by intercalated benzo[a]-pyrene diol epoxide adducts at the 6-amino group of adenine, Proc Natl Acad Sci U S A 97 (2000) 10739-10744.**

[18] **P. Pourquier, A.A. Pilon, G. Kohlhagen, A. Mazumder, A. Sharma and Y. Pommier Trapping of mammalian topoisomerase I and recombinations induced by damaged DNA containing nicks or gaps. Importance of DNA end phosphorylation and camptothecin effects, J Biol Chem 272 (1997) 26441-26447.**

[19] **K. Christiansen and O. Westergaard Mapping of eukaryotic DNA topoisomerase I catalyzed cleavage without concomitant religation in the vicinity of DNA structural anomalies, Biochim Biophys Acta 1489 (1999) 249-262.**

[20] **P. Pourquier, L.M. Ueng, J. Fertala, D. Wang, H.J. Park, J.M. Essigmann, M.A. Bjornsti and Y. Pommier Induction of reversible complexes between eukaryotic DNA topoisomerase I and DNA-containing oxidative base damages. 7, 8-dihydro-8-oxoguanine and 5-hydroxycytosine, J Biol Chem 274 (1999) 8516-8523.**

[21] **D.T. Lesher, Y. Pommier, L. Stewart and M.R. Redinbo 8-Oxoguanine rearranges the active site of human topoisomerase I, Proc Natl Acad Sci U S A 99 (2002) 12102-12107.**

[22] **L. Debethune, G. Kohlhagen, A. Grandas and Y. Pommier Processing of nucleopeptides mimicking the topoisomerase I-DNA covalent complex by tyrosyl-DNA phosphodiesterase, Nucleic Acids Res 30 (2002) 1198-1204.**

[23] **D.R. Davies, H. Interthal, J.J. Champoux and W.G. Hol The crystal structure of human tyrosyl-DNA phosphodiesterase, Tdp1, Structure (Camb) 10 (2002) 237-248.**

[24] **D.R. Davies, H. Interthal, J.J. Champoux and W.G. Hol Crystal structure of a transition state mimic for Tdp1 assembled from vanadate, DNA, and a topoisomerase I-derived peptide, Chem Biol 10 (2003) 139-147.**

[25] **K.V. Inamdar, J.J. Pouliot, T. Zhou, S.P. Lees-Miller, A. Rasouli-Nia and L.F. Povirk Conversion of phosphoglycolate to phosphate termini on 3' overhangs of DNA double strand breaks by the human tyrosyl-DNA phosphodiesterase hTdp1, J Biol Chem 277 (2002) 27162-27168.**

[26] **H. Interthal, H.J. Chen and J.J. Champoux Human Tdp1 cleaves a broad spectrum of substrates, including phosphoamide linkages, J Biol Chem 280 (2005) 36518-36528.**

[27] **H. Takashima, C.F. Boerkoel, J. John, G.M. Saifi, M.A. Salih, D. Armstrong, Y. Mao, F.A. Quiocho, B.B. Roa, M. Nakagawa, D.W. Stockton and J.R. Lupski Mutation of TDP1, encoding a topoisomerase I-dependent DNA damage repair enzyme, in spinocerebellar ataxia with axonal neuropathy, Nat Genet 32 (2002) 267-272.**

[28] **S.F. El-Khamisy, G.M. Saifi, M. Weinfeld, F. Johansson, T. Helleday, J.R. Lupski and K.W. Caldecott Defective DNA single-strand break repair in spinocerebellar ataxia with axonal neuropathy-1, Nature 434 (2005) 108-113.**

[29] **H. Interthal, H.J. Chen, T.E. Kehl-Fie, J. Zotzmann, J.B. Leppard and J.J. Champoux SCAN1 mutant Tdp1 accumulates the enzyme--DNA intermediate and causes camptothecin hypersensitivity, Embo J 24 (2005) 2224-2233.**

[30] **I. Plo, Z.Y. Liao, J.M. Barcelo, G. Kohlhagen, K.W. Caldecott, M. Weinfeld and Y. Pommier Association of XRCC1 and tyrosyl DNA phosphodiesterase (Tdp1) for the repair of topoisomerase I-mediated DNA lesions, DNA Repair (Amst) 2 (2003) 1087-1100.**

[31] **Z.H. Miao, K. Agama, O. Sordet, L. Povirk, K.W. Kohn and Y. Pommier Hereditary ataxia SCAN1 cells are defective for the repair of transcription-dependent topoisomerase I cleavage complexes, DNA Repair (Amst) 5 (2006) 1489-1494.**

[32] **J.E. Ward Nature of lesions formed by ionizing radiation, in: J.A. Nickoloff and M.F. Hoekstra (Eds.), DNA damage and Repair, Human Press, Totowa NJ, 1998, pp. 65-84.**

[33] **R. Teoule Radiation-induced DNA damage and its repair, Int J Radiat Biol Relat Stud Phys Chem Med 51 (1987) 573-589.**

[34] **J.F. Ward DNA damage produced by ionizing radiation in mammalian cells: identities, mechanisms of formation, and reparability, Prog Nucleic Acid Res Mol Biol 35 (1988) 95-125.**

[35] **M.O. Bradley and K.W. Kohn X-ray induced DNA double strand break production and repair in mammalian cells as measured by neutral filter elution, Nucleic Acids Res 7 (1979) 793-804.**

[36] **H.E. Bryant, N. Schultz, H.D. Thomas, K.M. Parker, D. Flower, E. Lopez, S. Kyle, M. Meuth, N.J. Curtin and T. Helleday Specific killing of BRCA2-deficient tumours with inhibitors of poly(ADP-ribose) polymerase, Nature 434 (2005) 913-917.**

[37] **H. Farmer, N. McCabe, C.J. Lord, A.N. Tutt, D.A. Johnson, T.B. Richardson, M. Santarosa, K.J. Dillon, I. Hickson, C. Knights, N.M. Martin, S.P. Jackson, G.C. Smith and A. Ashworth Targeting the DNA repair defect in BRCA mutant cells as a therapeutic strategy, Nature 434 (2005) 917-921.**

[38] **P.L. Olive, J.P. Banath and R.E. Durand Heterogeneity in radiation-induced DNA damage and repair in tumor and normal cells measured using the "comet" assay, Radiat Res 122 (1990) 86-94.**

[39] **A. Rapp and K.O. Greulich After double-strand break induction by UV-A, homologous recombination and nonhomologous end joining cooperate at the same DSB if both systems are available, J Cell Sci 117 (2004) 4935-4945.**

[40] **R. Fan, T.S. Kumaravel, F. Jalali, P. Marrano, J.A. Squire and R.G. Bristow Defective DNA strand break repair after DNA damage in prostate cancer cells: implications for genetic instability and prostate cancer progression, Cancer Res 64 (2004) 8526-8533.**

[41] **K.W. Caldecott, S. Aoufouchi, P. Johnson and S. Shall XRCC1 polypeptide interacts with DNA polymerase beta and possibly poly (ADP-ribose) polymerase, and DNA ligase III is a novel molecular 'nick-sensor' in vitro, Nucleic Acids Res 24 (1996) 4387-4394.**

[42] **K.W. Caldecott, J.D. Tucker, L.H. Stanker and L.H. Thompson Characterization of the XRCC1-DNA ligase III complex in vitro and its absence from mutant hamster cells, Nucleic Acids Res 23 (1995) 4836-4843.**

[43] **J.L. Shaw, J. Blanco and G.C. Mueller Simple procedure for isolation of DNA, RNA and protein fractions from cultured animal cells, Anal Biochem 65 (1975) 125-131.**

[44] **S. Keeney, C.N. Giroux and N. Kleckner Meiosis-specific DNA double-strand breaks are catalyzed by Spo11, a member of a widely conserved protein family, Cell 88 (1997) 375-384.**

[45] **M. O'Driscoll, K.M. Cerosaletti, P.M. Girard, Y. Dai, M. Stumm, B. Kysela, B. Hirsch, A. Gennery, S.E. Palmer, J. Seidel, R.A. Gatti, R. Varon, M.A. Oettinger, H. Neitzel, P.A. Jeggo and P. Concannon DNA ligase IV mutations identified in patients exhibiting developmental delay and immunodeficiency, Mol Cell 8 (2001) 1175-1185.**

[46] **J. Smith, E. Riballo, B. Kysela, C. Baldeyron, K. Manolis, C. Masson, M.R. Lieber, D. Papadopoulo and P. Jeggo Impact of DNA ligase IV on the fidelity of end joining in human cells, Nucleic Acids Res 31 (2003) 2157-2167.**

[47] **T. Zhou, J.W. Lee, H. Tatavarthi, J.R. Lupski, K. Valerie and L.F. Povirk Deficiency in 3'-phosphoglycolate processing in human cells with a hereditary mutation in tyrosyl-DNA phosphodiesterase (TDP1), Nucleic Acids Res 33 (2005) 289-297.**

[48] **J.L. Parsons, Dianova, II and G.L. Dianov APE1 is the major 3'-phosphoglycolate activity in human cell extracts, Nucleic Acids Res 32 (2004) 3531-3536.**

[49] **C. Liu, J.J. Pouliot and H.A. Nash Repair of topoisomerase I covalent complexes in the absence of the tyrosyl-DNA phosphodiesterase Tdp1, Proc Natl Acad Sci U S A 99 (2002) 14970-14975.**

[50] **H.F. Zhang, A. Tomida, R. Koshimizu, Y. Ogiso, S. Lei and T. Tsuruo Cullin 3 promotes proteasomal degradation of the topoisomerase I-DNA covalent complex, Cancer Res 64 (2004) 1114-1121.**

[51] **S.D. Desai, L.F. Liu, D. Vazquez-Abad and P. D'Arpa Ubiquitin-dependent destruction of topoisomerase I is stimulated by the antitumor drug camptothecin, J Biol Chem 272 (1997) 24159-24164.**

[52] **D.R. Beidler and Y.C. Cheng Camptothecin induction of a time- and concentration-dependent decrease of topoisomerase I and its implication in camptothecin activity, Mol Pharmacol 47 (1995) 907-914.**

[53] **S.D. Desai, H. Zhang, A. Rodriguez-Bauman, J.M. Yang, X. Wu, M.K. Gounder, E.H. Rubin and L.F. Liu Transcription-dependent degradation of topoisomerase I-DNA covalent complexes, Mol Cell Biol 23 (2003) 2341-2350.**

[54] **M.T. Tomicic, M. Christmann and B. Kaina Topotecan-triggered degradation of topoisomerase I is p53-dependent and impacts cell survival, Cancer Res 65 (2005) 8920-8926.**

[55] **P. Pourquier, L.M. Ueng, G. Kohlhagen, A. Mazumder, M. Gupta, K.W. Kohn and Y. Pommier Effects of uracil incorporation, DNA mismatches, and abasic sites on cleavage and religation activities of mammalian topoisomerase I, J Biol Chem 272 (1997) 7792-7796.**

[56] **J.E. Chrencik, A.B. Burgin, Y. Pommier, L. Stewart and M.R. Redinbo Structural impact of the leukemia drug 1-beta-D-arabinofuranosylcytosine (Ara-C) on the covalent human topoisomerase I-DNA complex, J Biol Chem 278 (2003) 12461-12466.**

[57] **P. Daroui, S.D. Desai, T.K. Li, A.A. Liu and L.F. Liu Hydrogen peroxide induces topoisomerase I-mediated DNA damage and cell death, J Biol Chem 279 (2004) 14587-14594.**

[58] **Y.H. Hsiang, R. Hertzberg, S. Hecht and L.F. Liu Camptothecin induces protein-linked DNA breaks via mammalian DNA topoisomerase I, J Biol Chem 260 (1985) 14873-14878.**

[59] **Y.H. Hsiang and L.F. Liu Identification of mammalian DNA topoisomerase I as an intracellular target of the anticancer drug camptothecin, Cancer Res 48 (1988) 1722-1726.**

[60] **J.Y. Chang, J.F. Liu, S.H. Juang, T.W. Liu and L.T. Chen Novel mutation of topoisomerase I in rendering cells resistant to camptothecin, Cancer Res 62 (2002) 3716-3721.**

[61] **K.C. Nitiss, M. Malik, X. He, S.W. White and J.L. Nitiss Tyrosyl-DNA phosphodiesterase (Tdp1) participates in the repair of Top2-mediated DNA damage, Proc Natl Acad Sci U S A 103 (2006) 8953-8958.**

[62] **W.D. Henner, L.O. Rodriguez, S.M. Hecht and W.A. Haseltine gamma Ray induced deoxyribonucleic acid strand breaks. 3' Glycolate termini, J Biol Chem 258 (1983) 711-713.**

[63] **S.F. El-Khamisy and K.W. Caldecott DNA single-strand break repair and spinocerebellar ataxia with axonal neuropathy-1, Neuroscience (2006).**

[64] **A. Barzilai, G. Rotman and Y. Shiloh ATM deficiency and oxidative stress: a new dimension of defective response to DNA damage, DNA Repair (Amst) 1 (2002) 3-25.**

[65] **T. Lu, Y. Pan, S.Y. Kao, C. Li, I. Kohane, J. Chan and B.A. Yankner Gene regulation and DNA damage in the ageing human brain, Nature 429 (2004) 883-891.**

[66] **C. Liu, S. Zhou, S. Begum, D. Sidransky, W.H. Westra, M. Brock and J.A. Califano Increased expression and activity of repair genes TDP1 and XPF in non-small cell lung cancer, Lung Cancer (2006).**

[67] **H. Interthal, J.J. Pouliot and J.J. Champoux The tyrosyl-DNA phosphodiesterase Tdp1 is a member of the phospholipase D superfamily, Proc Natl Acad Sci U S A 98 (2001) 12009-12014.**

[68] **T.J. Cheng, P.G. Rey, T. Poon and C.C. Kan Kinetic studies of human tyrosyl-DNA phosphodiesterase, an enzyme in the topoisomerase I DNA repair pathway, Eur J Biochem 269 (2002) 3697-3704.**

[69] **A.C. Raymond, B.L. Staker and A.B. Burgin, Jr. Substrate specificity of tyrosyl-DNA phosphodiesterase I (Tdp1), J Biol Chem 280 (2005) 22029-22035.**

Figure 1

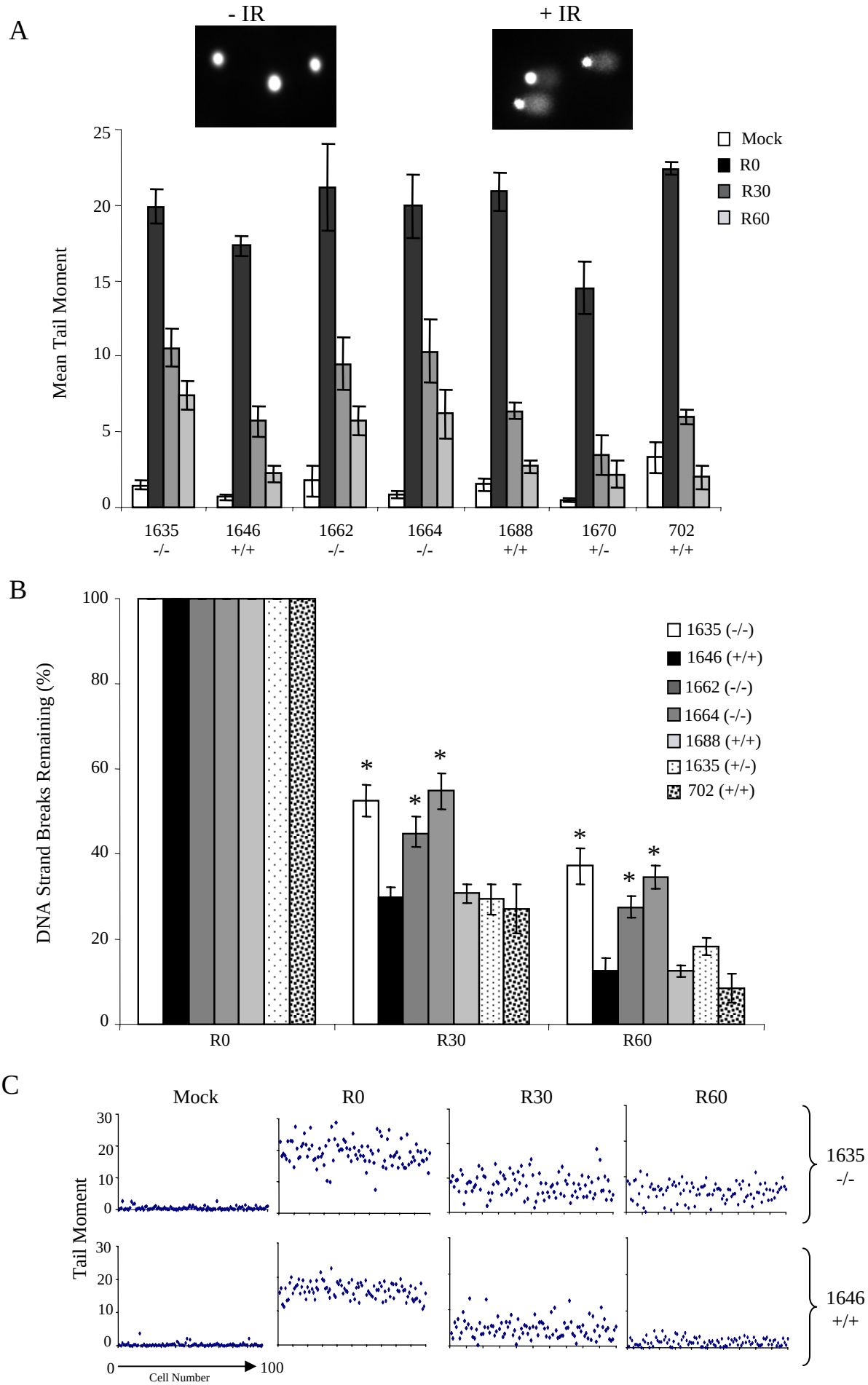
A
- IR
+ IR
Mean Tail Moment
25
20
15
10
5
0
Mock
R0
R30
R60
1635 -/-
1646 +/+
1662 -/-
1664 -/-
1688 +/+
1670 +/-
702 +/+
B
DNA Strand Breaks Remaining (%)
100
80
60
40
20
0
1635 (-/-)
1646 (+/+)
1662 (-/-)
1664 (-/-)
1688 (+/+)
1635 (+/-)
702 (+/+)
R0
R30
R60
C
Mock
R0
R30
R60
Tail Moment
30
20
10
0
1635 -/-
1646 +/+
0
Cell Number
100

Figure 2

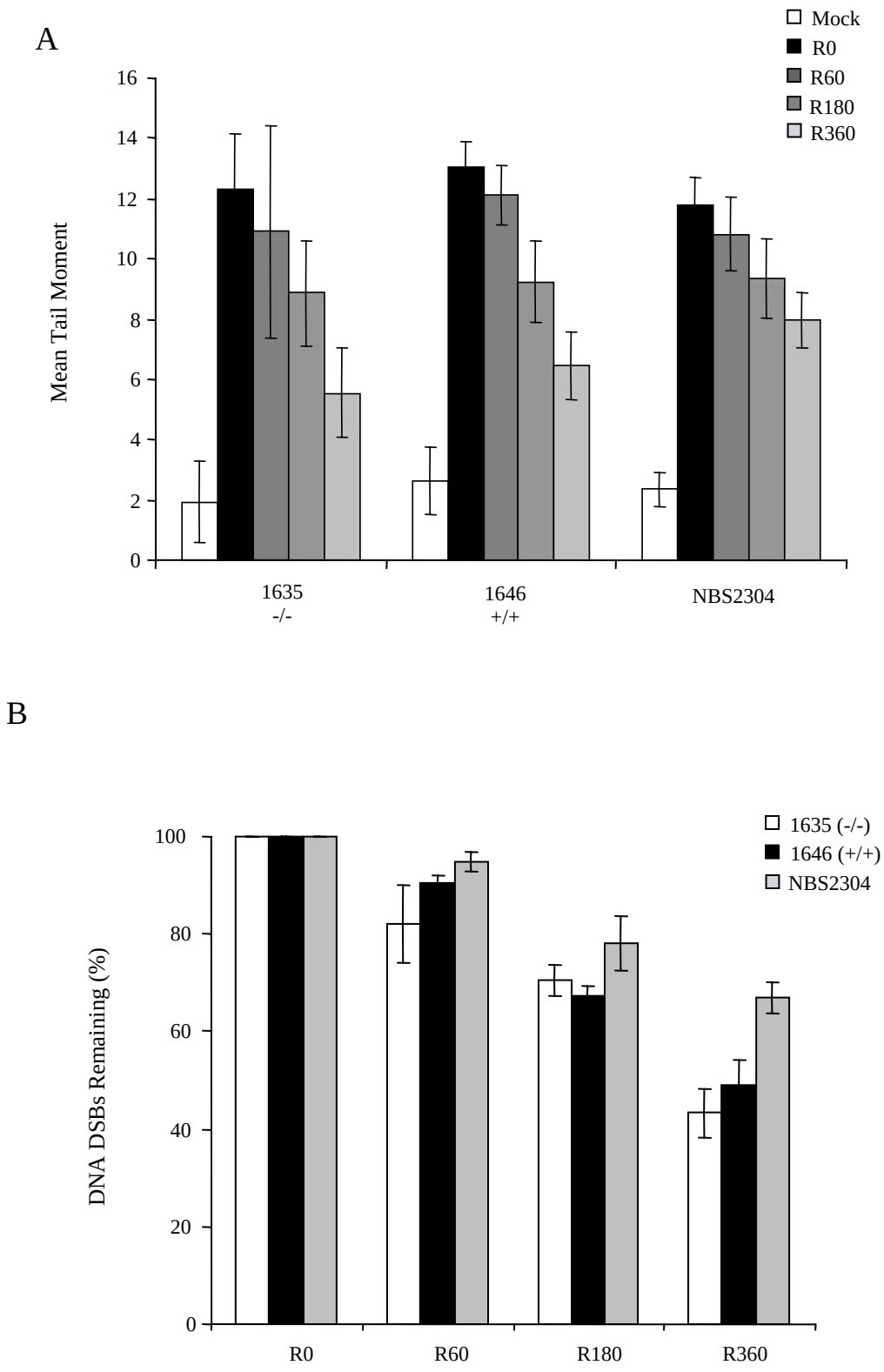
A
Mock
R0
R60
R180
R360
Mean Tail Moment
0
2
4
6
8
10
12
14
16
1635
-/-
1646
+/+
NBS2304
B
1635 (-/-)
1646 (+/+)
NBS2304
DNA DSBs Remaining (%)
0
20
40
60
80
100
R0
R60
R180
R360

Figure 3

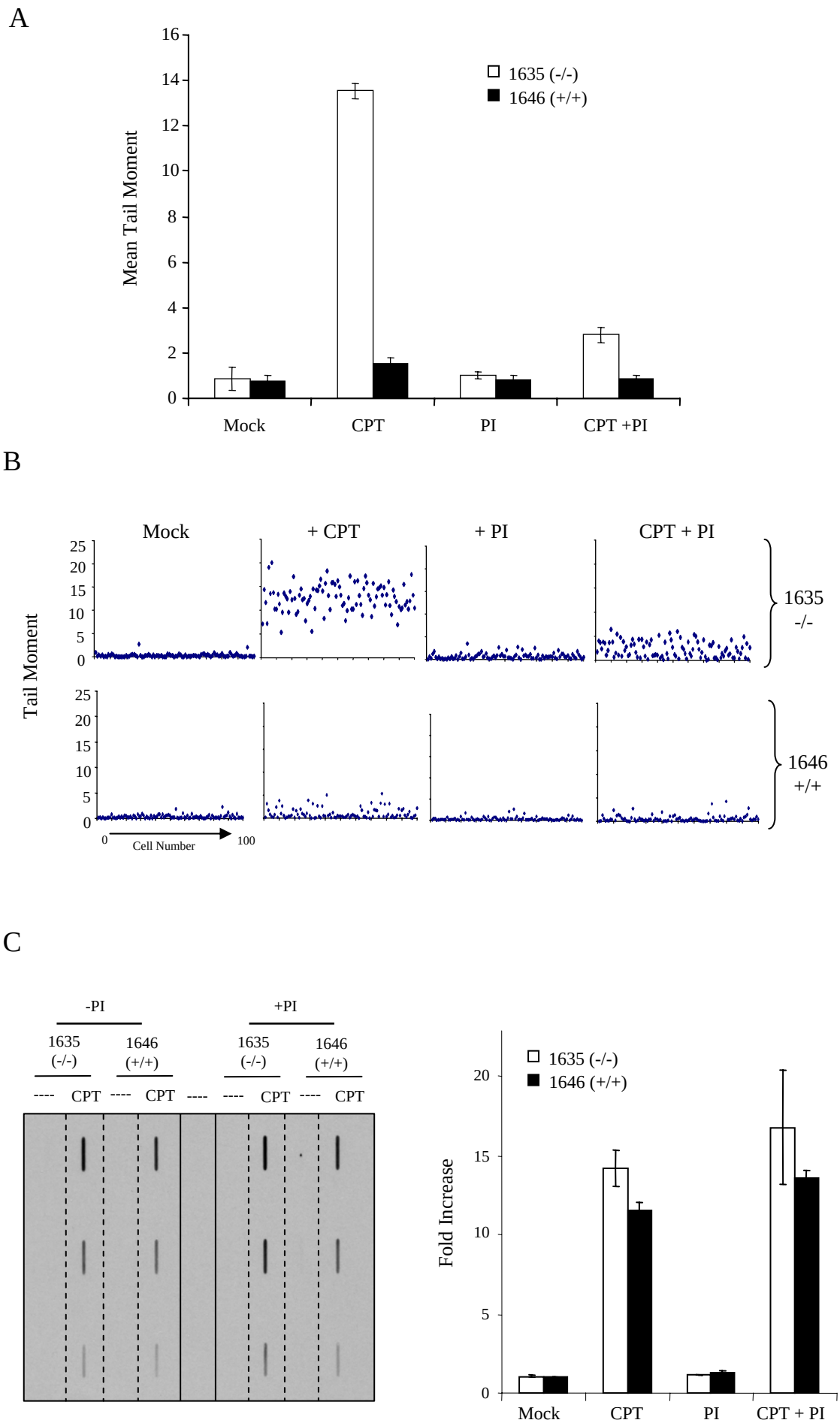
A
Mean Tail Moment
16
14
12
10
8
6
4
2
0
1635 (-/-)
1646 (+/+)
Mock
CPT
PI
CPT +PI
B
Mock
+ CPT
+ PI
CPT + PI
Tail Moment
25
20
15
10
5
0
1635
-/-
1646
+/+
0
Cell Number
100
C
-PI
+PI
1635
(-/-)
1646
(+/+)
1635
(-/-)
1646
(+/+)
---- CPT ---- CPT ---- ---- CPT ---- CPT
Fold Increase
20
15
10
5
0
1635 (-/-)
1646 (+/+)
Mock
CPT
PI
CPT + PI

Figure 4

A

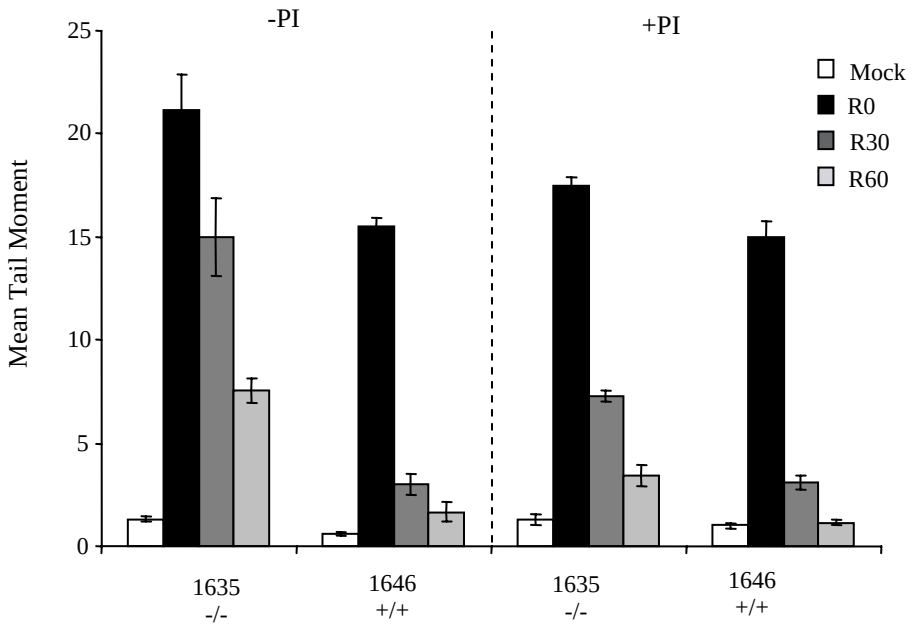
-PI
+PI
Mock
R0
R30
R60
Mean Tail Moment
25
20
15
10
5
0
1635
-/-
1646
+/+
1635
-/-
1646
+/+

B

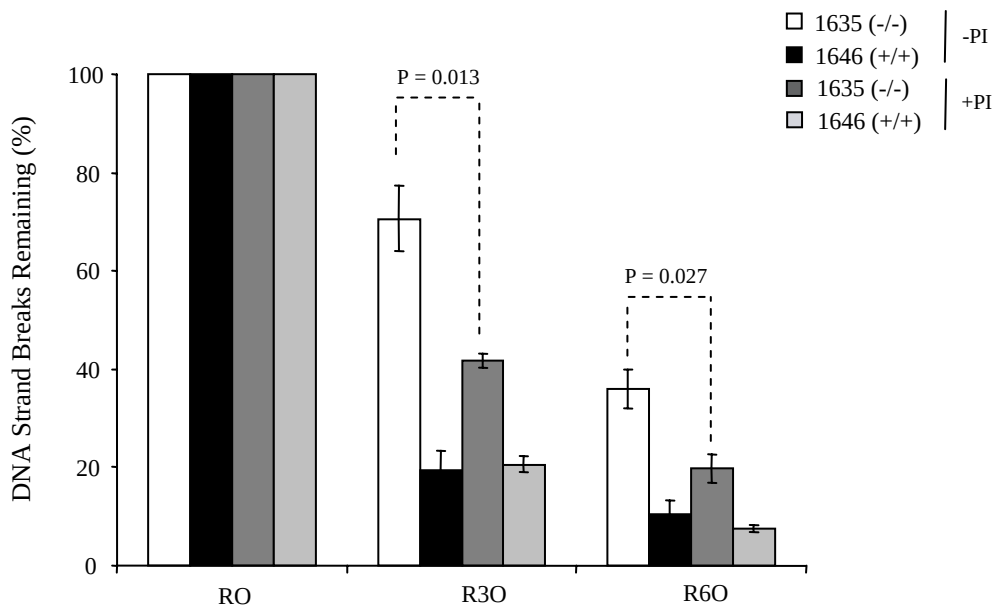
1635 (-/-)
1646 (+/+)
1635 (-/-)
1646 (+/+)
-PI
+PI
DNA Strand Breaks Remaining (%)
100
80
60
40
20
0
P = 0.013
P = 0.027
RO
R3O
R6O

Figure 5

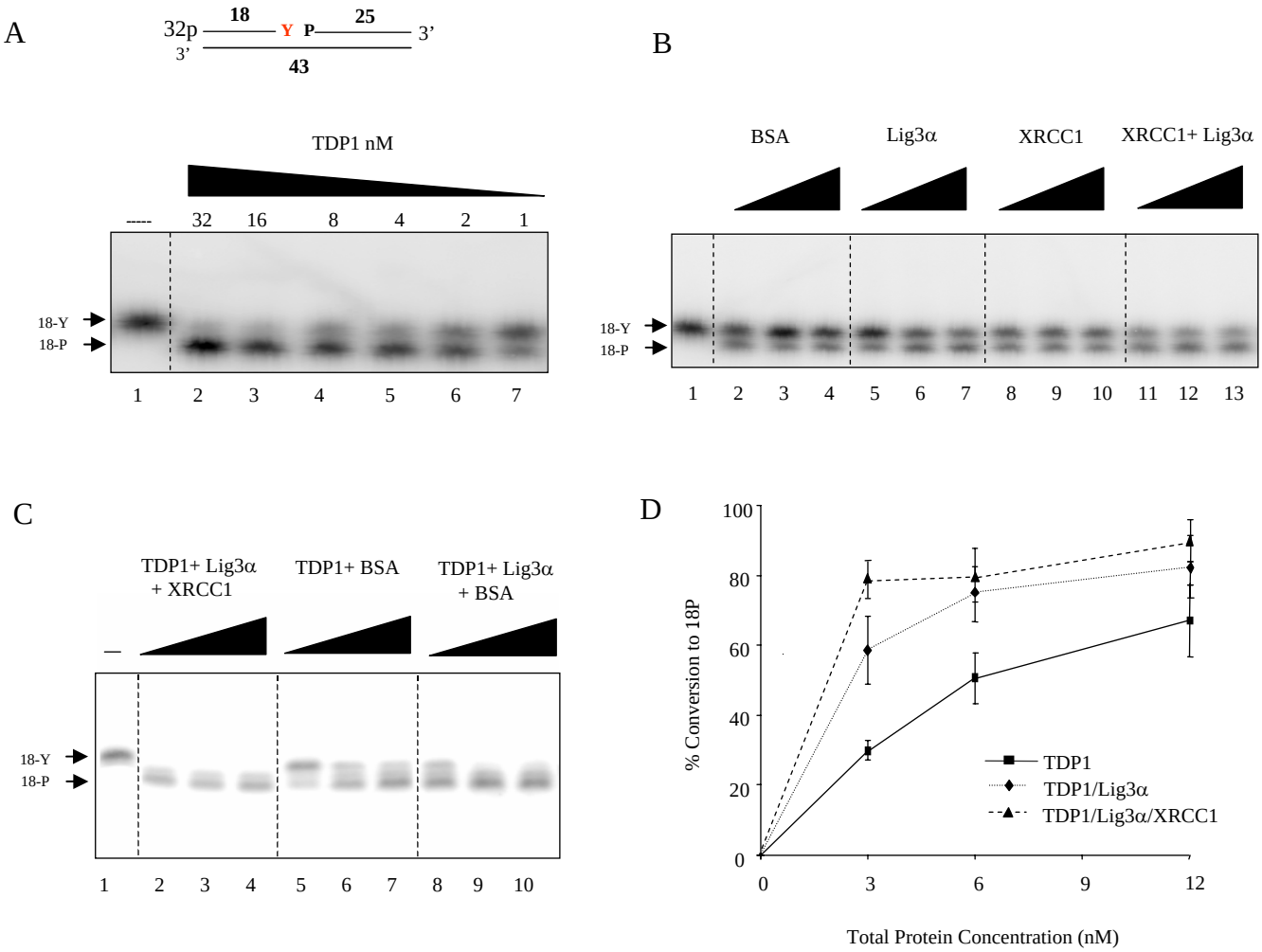
A
32p
18
Y
P
25
3'
3'
43
TDP1 nM

32
16
8
4
2
1
18-Y
18-P
1 2 3 4 5 6 7
B
BSA
Lig3α
XRCC1
XRCC1+ Lig3α
18-Y
18-P
1 2 3 4 5 6 7 8 9 10 11 12 13
C
TDP1+ Lig3α
+ XRCC1
TDP1+ BSA
TDP1+ Lig3α
+ BSA
—
18-Y
18-P
1 2 3 4 5 6 7 8 9 10
D
% Conversion to 18P
100
80
60
40
20
0
0 3 6 9 12
TDP1
TDP1/Lig3α
TDP1/Lig3α/XRCC1
Total Protein Concentration (nM)